International Journal of Hydrogen Energy 101 (2025) 47–53

Contents lists available at ScienceDirect

International Journal of Hydrogen Energy

journal homepage: www.elsevier.com/locate/he

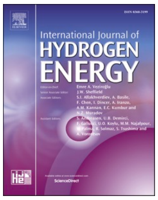

Hydrogen technologies: Optical properties of hydrogenated amorphous thin films for solar cells☆

Bakhtiyar A. Najafov [a], Shukur N. Nasirov [b,*], Shamsi N. Nasirov [c]

[a] *Institute of Radiation Problems of the Ministry of Science and Education, B. Vahabzade st., 9, Az 1143, Baku, Azerbaijan*
[b] *Azerbaijan State Oil and Industry University, Azadlig Ave., 16/21, Az 1010, Baku, Azerbaijan*
[c] *Baku Engineering University, st. Hasan Aliyev, 120, Az 0102, Khirdalan, Azerbaijan*

ARTICLE INFO

Keywords:
Hydrogen technology
Hydrogen
Hydrogenation
Oscillator
Absorption coefficient
Effusion of hydrogen
Deposition rate

ABSTRACT

Hydrogen technologies are rapidly penetrating all aspects of life, forming the basis of the Hydrogen Civilization of the future.

Hydrogenated amorphous silicon (a-Si:H) thin films are widely used in solar cells due to their advantageous optical properties. Here are some key points about their optical characteristics:

1. Optical Band Gap: The optical band gap of a-Si:H can be tuned by adjusting the hydrogen content during deposition. This allows for better absorption of sunlight and improved efficiency in solar cells.
2. Refractive Index: The refractive index of these films is crucial for designing anti-reflective coatings, which enhance the amount of light entering the solar cell.
3. Urbach Energy: This parameter indicates the width of the tail of localized states in the band gap. Lower Urbach energy values are desirable as they signify fewer defects and better electronic properties.
4. Absorption Coefficient: High absorption coefficients in the visible spectrum are essential for thin-film solar cells to absorb maximum sunlight with minimal material.
5. Hydrogen's Role: Hydrogenation helps in passivating dangling bonds in the silicon network, reducing defects and improving the material's optical and electronic properties.

These properties make hydrogenated amorphous silicon thin films a popular choice for cost-effective and efficient solar cells.

Infrared (IR) absorption spectra are investigated hydrogenated amorphous solid solution films a-Si$_{1-x}$Ge$_x$: H (x = 0 ÷ 1) plasma chemical vapor deposition at different partial pressures of hydrogen P_{H2}. Defined force, oscillator, which essentially depended on P_{H2}. It is shown that the hydrogen contained in films mostly in the forms of GeH, SiH. Using integrated acquisitions J_W, determined the amount of hydrogen in the films. Film properties depend on the composition and level of hydrogenation. The number of hydrogen atoms in films, varied by changing the composition of the gas mixture. In the work measured IR absorption for films a-Si$_{1-x}$Ge$_x$: H, a-Ge:H and a-Si$_{0,88}$Ge$_{0,\ 12}$: H based on films and a-Si: H and a-Si$_{0,88}$Ge$_{0,\ 12}$: H fabricated three-layer solar cells with an area of item 1.3 cm^2 and efficiency equal to ∼9.5%.

1. Introduction

The use of hydrogen technologies for the production of eco-energy objects is an important area of the Hydrogen Civilization concept. Hydrogen alloying additives allow for a significant improvement in the quality of objects in conveyor production conditions. Hydrogenated

---

☆ This paper is the English version of the paper reviewed and published in Russian in **"International Scientific Journal for Alternative Energy and Ecology". ISJAEE, 08, #425, (2024).**

* Corresponding author.
E-mail address: sh.nasirov62@inbox.ru (S.N. Nasirov).

https://doi.org/10.1016/j.ijhydene.2024.12.161
Received 27 November 2024; Accepted 8 December 2024

amorphous thin films, particularly hydrogenated amorphous silicon (a-Si:H), are crucial in the development of efficient solar cells. Here are some key points about their optical properties:

1. Optical Band Gap: The optical band gap of hydrogenated amorphous silicon can be tuned by varying the hydrogen content. This property is essential for optimizing the absorption of sunlight and improving the efficiency of solar cells [1].
2. Refractive Index and Extinction Coefficient: These films exhibit specific refractive indices and extinction coefficients that are wavelength-dependent. These optical constants are critical for designing anti-reflection coatings and enhancing light absorption [1].
3. Urbach Tail: The Urbach tail represents the exponential edge in the absorption spectrum of the material. It is influenced by the disorder in the amorphous structure and affects the material's optical absorption near the band edge [1].
4. Photoconductivity: Hydrogenated amorphous silicon films show significant photoconductivity, which is beneficial for their application in photovoltaic devices. This property is influenced by the quality of the film and the presence of defects [2].
5. Deposition Methods: Techniques such as Plasma Enhanced Chemical Vapor Deposition (PECVD) are commonly used to produce these films. The deposition method can impact the film's microstructure and, consequently, its optical properties [3].

Introduction of Si films and its alloy characterized by various structural phases. The most interesting of them are crystals that are in the amorphous matrix. Such alloys are produced by different methods at different technological regimes. For films of amorphous hydrogenated silicon and a-Si: H, formed by the method of cyclic sedimentation annealed in hydrogen plasma effect Staebler-Vronsky is expressed weakly [4]. Authors [5] note the absence of the effect of Staebler-Vronsky in Nano structural films of a-Si:H film Silicon alloys crystallization of a-Si: H is carried out by various methods: long annealing in vacuum at 600 °C, fast heat treatment [6], laser annealing [7] and ion implantation [8]. The mobility of the charge carriers, alloying and efficiency optical absorption coefficient in films of a-Si: H she than crystalline silicon. Films a-$Si_{1\text{-}x}Ge_x$: H are an effective and inexpensive material for making solar cells and other electronic devices [9,10].

In this regard, the receipt of the aforementioned films and changing their conductivity type are actual tasks [11]. shows that with the change in the temperature of the substrate grow Nano crystals increases. Found that with increasing concentration of average grain size decreases RN3 (d) and the proportion of crystalline particle volume (V_c). When alloying with increasing concentration of boron, B_2H_6, value (d) does not change, and V_c is reduced. The value of photo films and efficiency-Si1-xGex: H, somewhat lower than in a-Si: H [12,13]. With the changing conditions of technology and technological parameters of hydrogen deposited on various structural phases: microcrystalline, polycrystalline, Nano crystalline, etc. of energy conversion efficiency based on Schottky barrier in films of a-Si: H was 5.5%. Attempts have been made to obtain high efficiency solar cell (~9.0%) on the basis of a-$Si_{1\text{-}x}Ge_x$: H [14].

Most literature data show that when using amorphous silicon and Silicon–Germanium alloys in solar cells with multilayered or cascading structure have the greatest efficiency ~8.5% [15].

Based on the above stated the purpose of this work is to determine the amount of hydrogen in amorphous films method for optical solid solution a-$Si_{1\text{-}x}Ge_x$: H (x = 0–1) and manufacturing of solar cells based on them.

NOMENCLATURE

List abbreviations And designations		*V*	Volt
atm	Atmosphere	*W/cm* ^{2}	Watt on square centimeter
EPR	Electronic paramagnetic resonance	*T s*	Temperature substrates
HF, RF	High frequency, Radio frequency	*v*	Speed precipitation
IR	Infrared	*c*	Speed of light
MRP	method recoil protons		
c.u.a.	Coefficient useful actions	*n*	Indicator refractions
N H	Integral ratio maxima IR absorption	*Si*	Silicon
		Ge	Germanium
mm, microns	Millimeter, micrometer		
nk- *Si*	Nanocrystalline silicon	*N A*	Number Avogadro
α- Si:H	Amorphous hydrogenated films silicon	*J w*	Integral absorption fashion swings for films
nc-Si:H	Nanocrystalline films silicon	*N H*	Number atoms hydrogen
Si -H	Monohydride films		
$Si–H_2$	Dihydride complexes	*J S*	Integral absorption fashion stretching for each films
FOMD	Forces oscillator by method decomposition silane on constant current	*N s*	Number density spins
PAS	Photoacoustic spectroscopy	*R*	Reflection films
(MPCP)	By method plasma chemical precipitation	*T*	Transmission Sveta specified lengths waves
cm^3/sec	Cubic centimeters a second		
IR-21	Spectrometer	*d*	Thickness films
MRP	Method recoil protons	*e* *	Effective charge
nm	Nanometers		
Latin letters		*m*	Given weight dipole
E 0	Width prohibited zones	*R*	Radius spheres volume, V which there is a dipole
eV	Electron-volt		
Wt	Watt	*Greek letters*	
C	Carbon	*Δω*	Shift stripes absorption
H 2 + SiH 4, He + Ge *H 4*	Gas mixture	ε	Dielectric constant
W	Power	*ω*	Frequency oscillations
°*C*	Degree Celsius	*λ*	Length waves
CH 4	Methane	α	Coefficient absorption
H 2	Hydrogen		

2. Formulation of the problem

Thin films of a-$Si_{1\text{-}x}Ge_x$: H (x = 0–1) received plasma chemical deposition method using gas mixtures of $H_2 + SiH_4$, $H_2 + GeH_4$ in various proportions. Details on obtaining films shown in Refs. [14,15]. Plasma RF field created through mainly inductive coupling. Film thickness was 0.1 ÷ 1.0 μm. Measured absorption coefficient (α), refraction (n), reflection (R), (T), width of band gap (E_0) for each sample, using appropriate models [16.17]. Optical absorption at room temperature were studied by the method of [16–19] on spectrometer IRS-29.

3. Results and discussion

The hydrogen concentration in a-Si1-xGex:H films, (x = 0 ÷ 1) is determined using the method of Brodsky et al. [17–20]:

$$N=\frac{AN_A}{(Q/\xi)}\int\frac{\alpha(\omega)}{\omega}d\omega, \tag{1}$$

where N is the number of Avogadro and (ξ) the integral strength of the hydride with units cm^2/mole (Q/ξ) = 3.5. If the width of the absorption indicate through and center frequency ω*, ω_0, when $\Delta\omega/\omega_0 \leq 0.1$ after approximation with a tolerance of ±2%, equation (1) can be written as follows:

$$N = \frac{AN_A}{(Q/\xi)\omega_0}\int \frac{\alpha(\omega)}{\omega}d\omega\ ; \tag{2}$$

where is: $A = \frac{(1+2\varepsilon)^2\varepsilon^{\frac{1}{2}}}{9\varepsilon^2}$; ε-dielectric constant. For Si, ε = 12; Ge, ε = 16.

If equation (2) pre integral expression Retable A_S and $J_S = \int\limits_{\omega_S}\alpha(\omega)d\omega$ – the cumulative uptake of fashion stretching for each film, then in determining hydrogen concentration (N_H) get a general expression in abbreviated form:

$$N_H = A_S J_S\ ; \tag{3}$$

Coefficient A_S– for films *a*-Si:H, is in the field of fashion stretching 1,4 × 10^{20}sm^{-2}. Absorption coefficient (α) for these phones (2100sm^{-1}) is 8 × 10^{-1}÷3 × 10^{2}sm^{-1}. When this N_H = 7 × 10^{21}÷2,1 × 10^{22}sm^{-3}. For films *a*-Ge:H A_S = 1,7 × 10^{20}sm^{-2}. In films *a*-Si:H and *a*-Ge:H absorption frequencies 2000 and 1980 sm-1 is caused by fluctuations in the type of valence and absorption frequencies 630 и 570sm^{-1} oscillations of type bend (Fig. 1a and c).

Thus, for *a*-$Si_{1-x}Ge_x$:H the place has a significant overlap, which is observed in the spectrum of IR absorption for both bands stretching Ge:H (1980 sm-1) and Si:H (2000 sm-1), and for bending strips around the frequency 600 cm^{-1} (Fig. 1b) [5,12]. It is clear that equation (3), so did the links stretch fashion oscillating characterizes in films *a*-Si:H, *a*-Ge:H and *a*-$Si_{1-x}Ge_x$:H. Assess the relative binding hydrogen to hydrogenated amorphous *a*-$Si_{1-x}Ge_x$:H:

$$P = \left\{\frac{N_{Si-H}}{N_{Ge-H}}\right\}\frac{x}{1-x}\ ; \tag{4}$$

Where is N_{Si-H} и $N_{Ge\text{-}H}$ – hydrogen concentration in *a*-Si:H and *a*-Ge:H (cm^3). Equation (3) You can rewrite to fashion swings (wagging mode) films *a*-Si:H and *a*-Ge:H. Thus, the value of N_{Si-H} and $N_{Ge\text{-}H}$ are determined from equation (3) to fashion rocking in the following form:

$$N_H = A_W J_W\ ; \tag{5}$$

where is,

$$J_W = \int\limits_{\omega_w}\frac{\alpha(\omega)}{\omega}d\omega$$

the cumulative up take of fashion swinging for films *a*-Si:H and *a*-Ge:H. For specified films A_w = 1,6 × 10^{19}sm^{-2} and A_w = 1,1 × 10^{19}sm^{-3}, accordingly. Knowing $N_{Ge\text{-}H}$ (where, for films *a*-Ge:H, A_w = 1,6 × 10^{19} sm^{-2} and α = 5 × 10^1 sm^{-1}), calculate hydrogen concentration N_H in the film *a*-$Si_{1-x}Ge_x$:H in the words of:

$$N_H = N_{Ge-H}^{wag}\left\{\frac{\int\limits_{streets}\left(\frac{\alpha_1(\omega)}{\omega}\right)d\omega}{\int\limits_{streets}\left(\frac{\alpha_2(\omega)}{\omega}\right)d\omega}\right\}\ ; \tag{6}$$

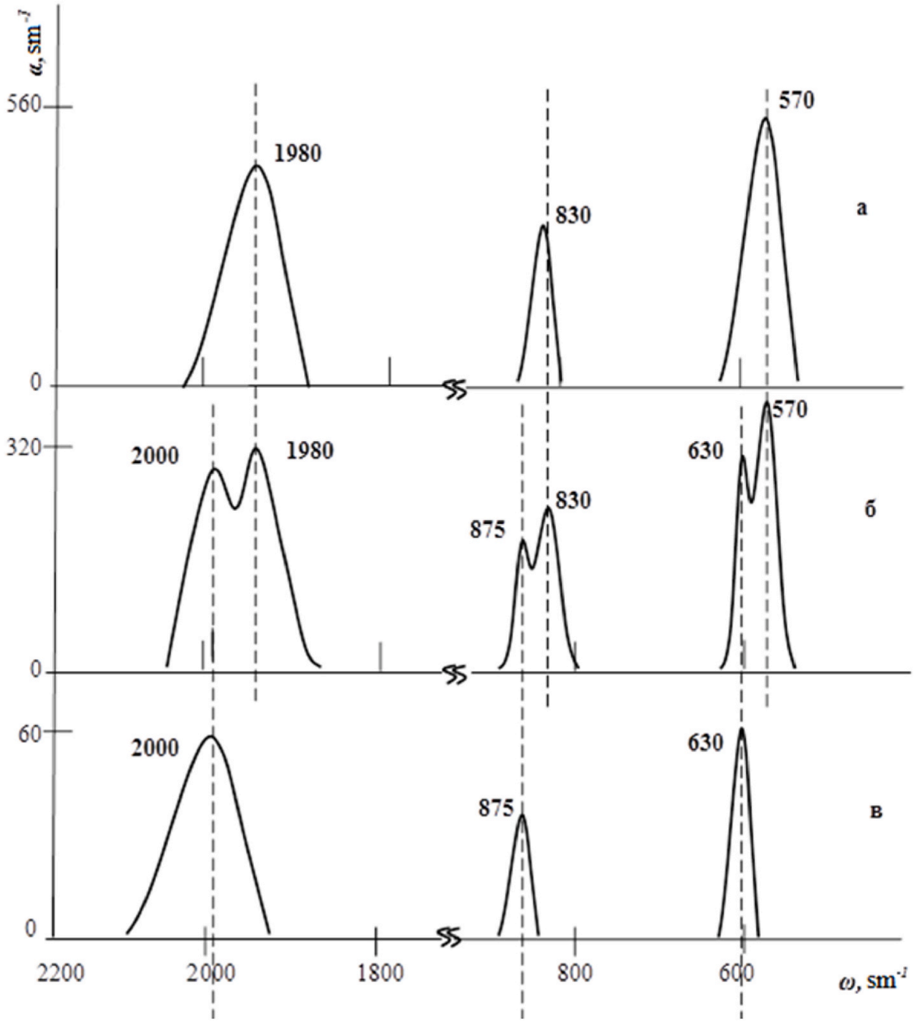

Fig. 1. INFRARED absorption Spectra of amorphous films of a-Si:H (a), a-$Si_{0,60}Ge_{0,40}$:H (b) and a-Ge: H (in) = 3.8 at mTorr. a-Si: H (s), a-Si0, 60Ge0, 40: (H) (b).

where is, N^{wag}_{Ge-H} – number of links Ge–H, some of the effects of net swing a-Ge:H, the value which, calculated according to equation (5). The second factor in the expression for N_H (cumulative ratio of IR absorption maxima) is a vibrational fashion stretching in the sample and in pure a-Ge:H. For the computation of the cumulative ratio used maximum satisfying the oscillatory fashion stretching Ge–H (2000 cm^{-1}) in the film a-$Si_{1-x}Ge_x$:H.

From these data it is possible to evaluate the effect of the oscillator in film a-$Si_{1-x}Ge_x$:H the ratio of:

$$Q = J_S / J_W,$$

where is,

$J_S \approx J^{Ge}_S + J^{Si}_S$, $J_W \approx J^{Ge}_W + J^{Si}_W$. Values $J^{Ge}_S, J^{Si}_S, J^{Ge}_W, J^{Si}_W$– are integrated acquisitions fashion, stretching and rocking, accordingly. The oscillator strength Q = 0,51 (for x = 0) and Q = 0,13 (for x = 1). The maximum value P = 4,16 for x = 0,40. Table 1 shows the characteristic parameters of amorphous films a-$Si_{0,60}Ge_{0,40}$:H on Fig. 2 shows the distribution of hydrogen on film thickness d: certain 1- method of recoil protons, 2- method of IR absorption spectrum. You can see, the distribution of hydrogen sufficiently uniform. Unlike other methods, the method of recoil protons (MRP) sample bombing beam of protons. When researching a-Si:H and its alloys, this allows you to get distribution hydrogen on thickness ~40 ÷ 100 Å. Method of calibration accuracy is limited only by the MCS, which is determined by the largest concentration of hydrogen (N_H), and IR spectroscopy of found values that match 2 ÷ 3 %.

This method provides information about the General content of both associated and not associated with Si hydrogen. A, with regard to the precise definition of hydrogen content in the volume of films, this band was analyzed infrared absorption 630 sm^{-1}. To clarify the amount of hydrogen is embedded in amorphous matrix below as follows is determined by the structural parameter (R):

$$R = \frac{J_{2000}}{J_{2000} + J_{2100}},$$

where is J_{2000} and J_{2100} – intensity of absorption bands at 2000 и 2100 sm^{-1}.

Using equation (3), of this ratio is determined by the concentration of hydrogen. Increase R occurs simultaneously with a decrease in the concentration of hydrogen. The highest magnitude R (before 0,8) observed for films a-Si:H, the besieged plasma chemical deposition method (PCDM), when T_S = 300^{0}C, power frequency discharge W = 100 W.

However, the films studied in the present work, that when T_S = 200 ÷ 300^{0}C, microstructure parameter cannot vary in the range R = 0,1 ÷ 0,8. When annealing during 30 min in a vacuum at R value reaches 1.0. Accordingly, in this case, C_H is 24.5 ÷ 14.0 at. %. By number of links Si–H, you can define a specific concentration of hydrogen containing links [Si–H]/[Si]. Specific concentrations of hydrogen containing Silicon links in the maximum reaches the value 0.58 [13–15].

Hydrogen concentration (N_H), some effusion method, correlated with the concentration of hydrogen, calculated using the integrated force I_W, fashion rocking 600 sm^{-1} (fiq. 3). The number of hydrogen atoms is found by at. % (C_H), effusion method is defined for the data tapes and compared to the number of hydrogen atoms N_A (Avogadro's number).

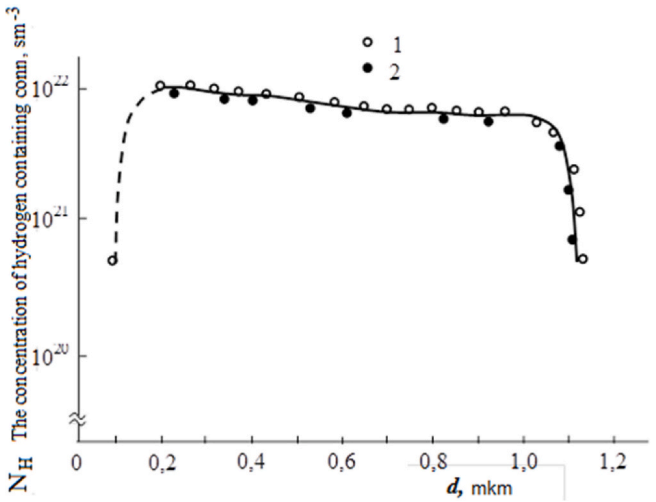

Fig. 2. distribution of hydrogen on thickness d some: 1-by-2 recoil protons by IR absorption spectrum.

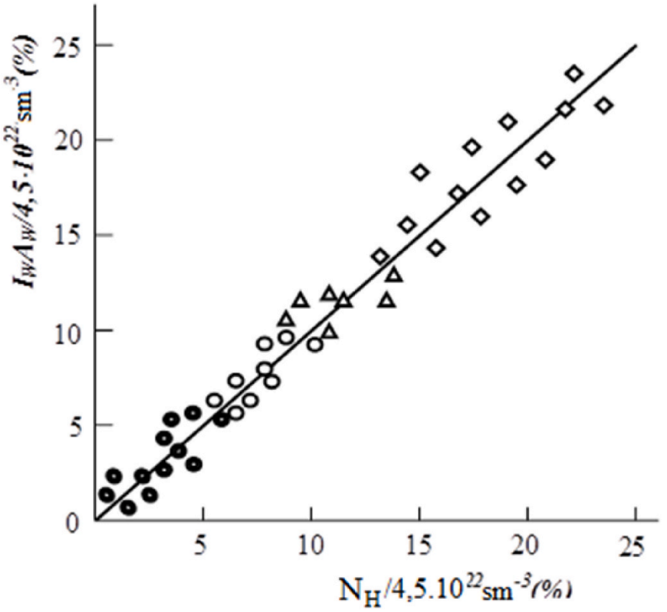

Fig. 3. Correlation of concentrations of hydrogen effusion method defined by the integrated force IW, at a frequency of 600 cM^{-1}-swing fashion 1, for films of a-$Si_{0,60}Ge_{0,40}$:H.

Therefore, the ratio of $\frac{J_W A_W}{N_H}$ compared to C_H (at. %) (Fig. 3).

Change C_H (at. %) for films at various temperatures heat up, shown in Table 1. Found that after effusion, during heat treatment up to 650 °C, hydrogen concentration is N_H = 1,3 at. %. In doing so, found that the

Table 1
Characteristic parameters of amorphous films a-$Si_{0,60}Ge_{0,40}$:H.

№ film	P_{H2},mTorr	E_0 eV	P	H at %	$N_{Si\bullet H}$ sm^{-3}	$N_{Ge\bullet H}$ sm^{-3}	N_H sm^{-3}	$I_S^{(Si)}$	$I_S^{(Ge)}$	$I_W^{(Ge)}$, $I_W^{(Si)}$	I_s/I_w
1	0,6	1,32	1,85	1,3	$6,2 \times 10^{21}$	$2,2 \times 10^{21}$	$3,1 \times 10^{20}$	$7,2 \times 10^{1}$	$6,3 \times 10^{1}$	$6,0 \times 10^{2}$	0,13
2	1,2	1,36	2,29	5,1	$9,4 \times 10^{21}$	$2,7 \times 10^{21}$	$4,0 \times 10^{21}$	$8,6 \times 10^{1}$	$7,5 \times 10^{1}$	$5,2 \times 10^{2}$	0,18
3	1,8	1,41	2,59	8,7	$1,3 \times 10^{22}$	$3,3 \times 10^{21}$	$5,1 \times 10^{21}$	$9,4 \times 10^{1}$	$8,3 \times 10^{1}$	$4,0 \times 10^{2}$	0,26
4	2,4	1,44	3,38	14,7	$2,1 \times 10^{22}$	$4,1 \times 10^{21}$	$6,2 \times 10^{21}$	$1,0 \times 10^{2}$	$9,0 \times 10^{1}$	$3,0 \times 10^{2}$	0,38
5	3,0	1,52	4,16	23,7	$2,9 \times 10^{22}$	$4,6 \times 10^{21}$	$9,7 \times 10^{21}$	$1,1 \times 10^{2}$	$1,0 \times 10^{2}$	$2,7 \times 10^{2}$	0,51

strength of the oscillator depend Q on hydrogen concentration (N_H), It decreases after effusion of hydrogen; with increased hydrogen content (P_{H2}) in the atmosphere of the received films *a*-$Si_{0,60}Ge_{0,40}$:H When partial pressures from 0.6 to 3.0 mTorr power oscillator increases [8, 15]. This is due to the hydrogen containing links Ge: H, Si:H at specified frequency.

Heating the sample in a closed volume is due to the fact that the material almost completely decomposed into its constituent elements, with crystallization temperature range 350 ÷ 650^0C, What causes hydrogen jeffuziju and leads to increased pressure. Pressure measured capacitive pressure gauge with a precision of 0,1 %. To determine the effusion other gases should undertake quantitative mass spectrometric analysis of the composition of the gas.

Note that the hydrogen inside the film identifies several ways: at. %, N_H, P_{H2} and P. To define these settings, you must remove the IR absorption spectra of the corresponding frequency fluctuations associated with the absorption of hydrogen.

Optical properties of thin films. The dependence of $(\alpha h\nu)^{1/2}$ from hν to determine the width of the forbidden zone [17,19] for each film.

In all the studied films of the optical absorption edge ratio describes the ratio of:

$$\alpha h\nu = B(h\nu - E_0)^2\,; \tag{7}$$

where is, $\alpha = 5 \times 10^4$ sm^{-1}, E_0 - optical band gap width for each film, B – the coefficient of proportionality. The value of the B determined by extrapolation of dependencies $(\alpha h\nu)^{1/2}$ from hν for each sample. Quadratic dependence (7) received in theory model, Describes the density of States slit mobility. The value of the B when x = 0 ÷ 1 at. %Ge, for films *a*-$Si_{1\text{-}x}Ge_x$:H changes from 527 before 343 $eV^{-1}cm^{1/2}$, accordingly, E_0 = 1,86 eV and E_0 = 1,14 eV. Means with increasing content of Germany, E_0 decreases. Mobility of carriers and photoconductivity in film *a*-$Si_{1\text{-}x}Ge_x$:H, also diminishes when Germany more 40 at.% [14,15]. We use the known relative absorption coefficient α-is determined from the following equation [17–20]:

$$T = \frac{(1-R_1)(1-R_2)(1-R_3)\exp(-\alpha d)}{(1-R_2R_3)\left\{1-\left[R_1R_2 + R_1R_2(1-R_2)^2\right]\right\}\exp(-2\alpha d)}\,; \tag{8}$$

here take, that

$$\begin{aligned} R_1 &= \left|(n-1)^2 + k_0^2\right| / \left|(n+1)^2 + k_0^2\right| \\ R_2 &= \left|(n-n_1)^2 + k_0^2\right| / \left|(n+n_1)^2 + k_0^2\right|\,; \\ R_3 &= \left|(n_1-1)\right| / \left|(n_1+1)\right|^2 \end{aligned} \tag{9}$$

For weakly absorbing light areas $k_0^2 \leq (n - 1, 5)$. κ_0 shows light attenuation in the substrate. Note that the film thickness d, defined in this case, the relevant transmission or reflection from extreme interference fringes.

From equation (8), the coefficients of absorption (α) are defined as follows:

$$T = \frac{kx}{a(1-bx)^2}$$

$$\left.\begin{aligned} &aT(1-bx)^2 = kx, \\ &k(1-R_1)(1-R_2)(1-R_3), \\ &a = 1 - R_2R_3, \\ &b = R_1R_2 + R_1R_3(1-R_2)^3, \\ &m = aTb, n = aT, \\ &mx^2 + kx - n = 0. \end{aligned}\right.\;; \tag{10}$$

$$\text{Then,} = \frac{1}{d} \cdot \frac{2m}{k \pm \sqrt{k^2 + 4mn}}\,; \tag{11}$$

Equation (11) is a working formula for determining optical absorption coefficients for films, in a weakly absorbing spectral region.

In a strongly absorbing spectral region R_3 = 0, R_2=R_1=R, n(λ) = const and n = n_1 = 1.5 for glass substrates, a n = n_1 = 3,42 for silicon substrate. Then equation (8) can be rewritten as follows:

$$T = \frac{(1-R)^2 e^{-\alpha d}}{1 - R^2 e^{-2\alpha d}}\,; \tag{12}$$

$$x = e^{-\alpha d};\; x^2 = e^{-2\alpha d};\; T = \frac{(1-R)^2 x}{1 - R^2 x^2}\,;$$

Then,

$$p = \frac{(1-R)^2}{T};\; \alpha = \frac{1}{d}\ln\left[\frac{1}{2}\left(\sqrt{p^2 + 4R^2} + p\right)\right]. \tag{13}$$

This formula can be used to determine the coefficient of optical absorption in a strongly absorbing spectral regions. Accordingly, the coefficients of refraction is defined using the following ratio:

$$nd = \frac{\lambda_m \lambda_{m-1}}{2(\lambda_{m-1} - \lambda_m)}$$

or by using the following formula:

$$\Delta n = \frac{c}{2\pi^2}\int \left[\frac{\alpha(\nu)}{\nu^2}\right] d\nu\,; \tag{14}$$

where is λ_m, $\lambda_{m\text{-}1}$ – the wavelength corresponding to the neigh boring extreme and spectra of transparency or reflection (corresponding frequency, c-the speed of light. Refractive index is defined or the following formula [18]:

$$n(\lambda) = \left[\left(\frac{2n_1(T_{\max} - T_{\min})}{T_{\max}T_{\min}} + \frac{n_1^2 + 1}{2}\right) + \sqrt{\left(\frac{2n_1(T_{\max} - T_{\min})}{T_{\max}T_{\min}} + \frac{n_1^2 + 1}{2}\right)^2 - n_1^2}\right]^{\frac{1}{2}}$$

where is T_{max} and T_{min} – functions of the wavelength λ, n_1– index of refraction of the substrate, which is defined by the expression:

$$n_1 = \frac{1}{T_1} - \sqrt{\frac{1}{T_1^2} - 1},$$

where is T_1 – deletion of the substrate, which is almost always in the area of transparency. As for glass substrates T_1 = 0,91, то n_1 = 1554.

Accordingly, the film thickness is calculated by the formula:

$$d = \frac{A\lambda_1\lambda_2}{2[n(\lambda_1\lambda_2) - n(\lambda_2\lambda_1)]},$$

where is λ_1 и λ_2 – wavelengths which correspond to the neigh touring extreme points on the spectrum bandwidth, A = 1 for two extremes of the same type (max– max, min– min) and A = 0,5 for two adjacent extremums of the opposite type (max– min, min– max).

Creation of solar cells. Studies show that films *a*-$Si_{1\text{-}x}Ge_x$:H ($x \geq 0{,}20$) can be used as a qualitative material in semiconductor electronics [15]. For this purpose we have developed a 3-item based on two elements of cascade type. Three-layer element is made of 2-layer element consisting of two elements on the basis of *a*-Si:H c *p-i-n* transition and *p-i-n* element with *i-a* layer of film *a*-$Si_{0,88}Ge_{0,12}$:H. The thickness i-layers to the top two transitions selected in such a way that respected the condition of equality of short-circuit current lower element. Short circuit current was about half the value for an element with a p-i-n transition. Idling voltage and short circuit current decreases with increasing number of superimposed layers. This way you can build multiple layers (create n-layer element). Note that for each item produced i-0.5 μm thick layer. The area of each element was 1.3 sm^2. When receiving a three-layer solar cells must be respected uniform thickness and square to each element. Substrate material of steel and was chosen as the cover used ZrO_2 with missing light 80%. Covering the same time playing the role of upper

ZrO_2 (front) of the contact. The thickness of the layers of a-Si: Hp-and n-types was ~300 and 400 Å, respectively. For alloying films number of B_2H_6 and PH_3 in gas mixtures changed within Alloy films in gas mixtures changed within 0.1 and 0.5%, respectively. After the deposition of amorphous semiconducting layers deposited by evaporation film ZrO_2 thickness ~500 Å. The upper contacts used Ni/Ag, for lower-stainless steel substrate. Items covered source sunlight provided AM-1 (100 mW/sm^2). Short-circuit current for 3-layer elements was 8,5 mA/sm^2, no-load voltage ~2,25 V, fill factor ~0,50 and CPA ~9,5% (fiq.4). CPA for single-layer and double-layer element is 7% and 8.9%, respectively. The effectiveness of collecting media when different wavelengths is defined by the formula:

$$Y(\lambda)=\frac{J_{Ph}(\lambda)}{eN(\lambda)}, \tag{15}$$

where is $J_{Ph}(\lambda)$ – the photocurrent density (10 mA/cm^2), N(λ) – the number of photons incident per unit surface per second, e−free media charge.

For elements with the structures of the short-circuit current is calculated in the supposition of a complete depletion of all layers, in the absence of direct bias. Thus, the short circuit current for the first, second, and third elements provides the following expressions:

$$I_{Sc3}=q\int_0^{1{,}24/E_{03}} \begin{matrix}(1-R)N_{ph}\exp\left(-3\alpha_n W_n-2\alpha_n W_n-2\alpha_p W_p-\alpha_1 W_1-\alpha_2 W_2\right)\\ [1-\exp(-\alpha_3 W_3)]d\lambda\end{matrix} \times \tag{16}$$

where is, W_i, W_n, W_p field distribution inside the i, n, p layer, respectively, N_{ph} – the number of photons incident on the surface of the elements, R – reflectivity film, α – absorption coefficient for each layer elements.

Idling voltage for cascading elements with two and three transitions is presented as:

$$V_{oc}(//)=0,5(E_{01}+E_{02}) \tag{17}$$

$$V_{oc}(III)=0,5(E_{01}+E_{02}+E_{03}) \tag{18}$$

The fill factor for all elements of the set size 0.5. Short-circuit current of a cascading element with two sets of values less transitions $I_{sc}(II)$ sets the lower value I_{sc1} and I_{sc2}. Short-circuit current of a cascading element with three passages is determined by the smallest amount of I_{sc1}, I_{sc2}, I_{sc3}.

CPA of many transitional cascade elements is given by the expression:

$$\eta(i)=0,5\cdot 0,5\left(\sum_i E_{0i}\right)\frac{I_{sc}(i)}{P_{in}} \tag{19}$$

where is i = 2 and 3 – shows the number of layers, P_{in} – power of incident light to the surface elements, its value is 100 mV/sm^2, E_{01}, E_{02}, E_{03} – Accordingly, the width of the forbidden zone for each i-the layer.

To raise η for solar cell, you want to increase the number of layers reduce the area elements, the choice of metal wires to reduce the resistance of the metal contacts, etc. Measurement of spectral sensitivity is usually produced at a constant illumination with white light, the intensity of which corresponds to the normal conditions of work (AM-1~100 mW/sm^2), at the same time an element falls modulation calibrated monochromatic radiation. Photocurrent and its dependence on wavelength of monochromatic radiation is measured in shorted circuits by using synchronized amplifier. To determine the effectiveness of collecting important knowledge of the electric field which is passed to the element. It has been noticed that in device dependently to the configuration collection efficiency is offset from red light in the blue spectrum.

It is known that the photon energy and momentum of the corresponding electromagnetic wave with frequency and wavelength in vacuum, equal:

$$W=h\nu=\frac{hc}{\lambda}\ ;\ P^*=\frac{h\nu}{c}=\frac{h}{\lambda},$$

where is, h - Planck's constant. When agile frequencies ν - the preponderant role played by wave properties, at large ν- particle properties of light. If P*- electromagnetic radiation energy feeding okay on some surface unit area for 1 s, c-the speed of propagation of light waves in a vacuum, R-reflectivity surface pressure p-light on this surface as well:

$$P=(1+R)N\frac{h\nu}{c}=P^*\Big/c(1+R) \tag{20}$$

light pressure (P) is defined by equation (19) and represent

$$P^*=\frac{W}{S}=\frac{hc}{\lambda S}\frac{N}{t}, \tag{21}$$

N- the number of incident photons. W- photon energy falling at all wavelengths of the body surface. P* -momentum light falling on dies surface for 1 s. Then the pressure of the incoming light is defined in the following form:

$$\begin{gathered} F=P\cdot S\\ F=\frac{hcNS(1+R)}{\lambda Stc}=\frac{hN(1+R)}{\lambda t}\\ F\lambda t=hN(1+R)\\ N=\frac{F\lambda t}{h(1+R)}, \end{gathered} \tag{22}$$

F - the power of light pressure (F = 10^{-8}H) on the surface (S = 1sm^2), λ-incident wave length, t-time of incidence of the light for 1 s with energy P* and its value is Nhν photons, with the momentum of each photon is equal to hν/c. With radiation reflection R, λ-the number falling photon is $10^{17}\div10^{18}$ m^{-2}s^{-1}, λ = 300 ÷ 900 nm.

4. Result

Obtained thin films a-$Si_{1-x}Ge_x$:H (x = 0 ÷ 1) plasma-chemical deposition method using gas mixtures of H_2 + SiH_4; H_2+GeH_4 in various proportions. It was determined that the highest R value (up to 0.8) is observed for films of a-Si:H deposited method (PHO) at temperature t = 300 °C, with an output frequency of discharge W = 100 W. The data on the ratio of $G=\frac{I_S}{I_W}$ the oscillator strength in the film was evaluated a-$Si_{1-x}Ge_x$:H, $I_S=I_S^{Ge}+I_S^{Si};\ \ I_W=I_W^{Ge}+I_W^{Si}$. Oscillator strength Q = 0,51 (for x = 0) and Q = 0,13 (for x = 1). For x = 0,40 maximum value P = 4,16. Based on the films a-Si:H and a-$Si_{0,88}Ge_{0,12}$:H manufactured solar cells and created single-layer, double-layer and three-layer structure; their characteristics are measured. Found that for single-layer, double-layer and three-layer structures with an area element 1,3 sm^2 η is 7 %; 8,9%; 9,5%, accordingly. For the three-layered element highs move in the scope of collection efficiency of longer wavelengths. In the reporting structures of their light in the wavelength interval 0,3 ÷ 1,1 μm within 120 h, there has been no degradation.

It is shown that the multi-layer structure solar cells based on a-$Si_{0,88}Ge_{0,12}$:H and a-Si:H effective, and the improvement of their efficiency are relevant tasks.

5. Conclusion

Hydrogen technologies are increasingly penetrating our lives, creating a serious foundation for the creation of the foundations of the Hydrogen Civilization of the future (Fig. 4).

In the course of the study, a number of works devoted to doping amorphous films with hydrogen were studied. Here are several well-known international scientific works devoted to the study of the optical properties of hydrogenated amorphous thin films for solar cells

Fig. 4. Hydrogen technologies in the production process of solar cells from amorphous silicon. (*provided to the authors on November 26, 2024 for printing in IJHE from the archive of Fermaltech Montenegro Limited, made by A.L. Gusev using Designer. On the DALL E 3 platform.)*. (For interpretation of the references to colour in this figure legend, the reader is referred to the Web version of this article.)

[21–24]. These works cover various aspects of the study of hydrogenated amorphous thin films, including their structural and optical properties, manufacturing methods and application in solar cells.

Interesting studies in a related field, important for understanding the role of hydrogen, were carried out during the work on the creation of hydrogen sensors [25–27]. Hydrogenated amorphous silicon (a-Si:H) thin films are widely used in solar cells due to their advantageous optical properties. Here are some key points about their optical characteristics:

1. Optical Band Gap: The optical band gap of a-Si:H can be tuned by adjusting the hydrogen content during deposition. This allows for better absorption of sunlight and improved efficiency in solar cells.
2. Refractive Index: The refractive index of these films is crucial for designing anti-reflective coatings, which enhance the amount of light entering the solar cell.
3. Urbach Energy: This parameter indicates the width of the tail of localized states in the band gap. Lower Urbach energy values are desirable as they signify fewer defects and better electronic properties.
4. Absorption Coefficient: High absorption coefficients in the visible spectrum are essential for thin-film solar cells to absorb maximum sunlight with minimal material.
5. Hydrogen's Role: Hydrogenation helps in passivating dangling bonds in the silicon network, reducing defects and improving the material's optical and electronic properties.
   These properties make hydrogenated amorphous silicon thin films a popular choice for cost-effective and efficient solar cells.

Infrared (IR) absorption spectra are investigated hydrogenated amorphous solid solution films a-$Si_{1-x}Ge_x$: H ($x = 0 \div 1$) plasma chemical vapor deposition at different partial pressures of hydrogen P_{H2}. Defined force, oscillator, which essentially depended on P_{H2}. It is shown that the hydrogen contained in films mostly in the forms of GeH, SiH. Using integrated acquisitions J_W, determined the amount of hydrogen in the films. Film properties depend on the composition and level of hydrogenation. The number of hydrogen atoms in films, varied by changing the composition of the gas mixture. In the work measured IR absorption for films a-$Si_{1-x}Ge_x$:H, a-Ge:H and a-$Si_{0,88}Ge_{0,\ 12}$: H based on films and a-Si: H and a-$Si_{0,88}Ge_{0,\ 12}$: H fabricated three-layer solar cells with an area of item 1.3 cm^2 and efficiency equal to ~9.5%.

Declaration of competing interest

There is no conflict of interest among the members of the authors' collective; the authors made an equal contribution to the work.

Acknowledgements

The work was presented at the Eighth World Congress on Alternative Energy and Ecology WCAEE-2024.

References

[1] https://cmsoep.physics.sjtu.edu.cn/doc/2006/JApplPhys_100_073516.pdf.
[2] https://www.scientific.net/AMR.1116.59.
[3] https://www.scientific.net/AMR.1116.59.
[4] [1] Yan Wang, Han Xiaoyan, Zhu Feng, HouGuofu, RenHuizhi J. Non- crystalline solids, vols. 9–20; 2006. p. 1909–12.
[5] Shimazaki K, Imaizumi M. Japon Atomic Energy Agency 2007;42:5.
[6] Neretina S, Sochinskii NV, Mascher PJ. J Electron Mat 2006;34(6):786–90.
[7] Stanimirova TJ, Atanasov PA, et al. J Appl Surface Sci 2007;253(19):8206–9.
[8] Chen Chao, Yu-zhen Liu, Cuo-bin Zhang, et al. J Luminescence 2007;28(4):579–84.
[9] Matsui T, Ogata K, Isomura M, Kondo M. J Non-Cryst Solids 2006;352(No 9–20): 1255–8.
[10] Najafov BA. Int J Appl Funda Res 2016;(7):61–73.
[11] Najafov BA, Fiqarov VR. Int J Hydrogen Energy 2010;35:4361–7.
[12] Guchiro Uchida, Sato Muneharu, SeoHyunwoong. Thin Solid Films 2013;v. 544: 93–8.
[13] Sachenko A, Korbutyak DV, Kryuchenko Yu. Nanoelectr Opto Electr 2011;6(4): 420–6.
[14] Najafov BA, Isakov GI. Isjaee. 2007. p. 177–8. No 11.
[15] Najafov BA, Abasov FP. Optoelectronic thin film processes and prospects of application. LAP, ГерМания 2015:433.
[16] Beams VV, Solovan M. FTT 2014;56(10).
[17] Najafov BA, Isakov GI. J Appl Spectrosc 2005;72(3):371–6.
[18] Najafov BA, Isakov GI. Inorg Mater 2010;46(6):624–30.
[19] Najafov BA, Abasov FP. Photonics. Ross 2014;44(2):72–90.
[20] Najafov BA. Int J Appl Fund Res 2016;12:1613–7.
[21] A. Barhdadi, M. Chafik El Idrissiю On the Structural and Optical Properties of Sputtered Hydrogenated Amorphous Silicon Thin Films" - https://arxiv.org/pdf/cond-mat/0208601.pdf.
[22] Ying Zhao, Xiaodan Zhang, Baojie Yan, Hydrogenated Amorphous Silicon Thin Film"- https://link.springer.com/referenceworkentry/10.1007/978-3-662-56472-1_27.
[23] Simulation and Fabrication of a-Si:H Thin-Film Solar Cells: A Comprehensive Study" https://link.springer.com/article/10.1007/s10854-024-12149-8.
[24] Hydrogen Technologies: Recent Advances, New Perspectives, and Applications" https://www.intechopen.com/chapters/1183330.
[25] Gusev AL, Zolotukhin IV, Kalinin Yu E, Korotkov LN, Samokhina OI, Sitnikov AV, Spiridonov BA. Effect of hydrogen on the electrical properties of silicon-doped metal oxides films. AEE; 2002. №6. URL: https://cyberleninka.ru/article/n/effects-of-hydrogen-on-electrical-properties-of-metal-oxide-films-alloy-silicon. [Accessed 27 November 2024].
[26] Gusev AL, Zolotukhin IV, Kalinin Yu E, Sitnikov AV, Stogney OV. Nanogranular structures as sensors for hydrogen and other gases. AEE; 2000. No1. URL: https://cyberleninka.ru/article/n/nanogranulirovannye-structure-kak-sensory-vodoroda-i-drugih-gazov. [Accessed 28 November 2024].
[27] Gusev AL, Zolotukhin IV, Kalinin Yu E, Korotkov LN, Samokhina OI, Sitnikov AV, Spiridonov BA. Hydrogen influence on electrical properties of metal oxide films alloyed with silicon. АЭЭ; 2003. NoS2. URL: https://cyberleninka.ru/article/n/influence-of-hydrogen-on-electrical-properties-of-metal-oxide-films-alloyed-with-silicon. [Accessed 28 November 2024].